

Analysis of composite steel-concrete beams using a refined high-order beam theory

M. Lezgy-Nazargah* and L. Kafi

Department of Civil Engineering, Hakim Sabzevari University, Sabzevar, Iran

(Received July 02, 2014, Revised November 18, 2014, Accepted November 24, 2014)

Abstract. A finite element model is presented for the analysis of composite steel-concrete beams based on a refined high-order theory. The employed theory satisfies all the kinematic and stress continuity conditions at the layer interfaces and considers effects of the transverse normal stress and transverse flexibility. The global displacement components, described by polynomial or combinations of polynomial and exponential expressions, are superposed on local ones chosen based on the layerwise or discrete-layer concepts. The present finite model does not need the incorporating any shear correction factor. Moreover, in the present C^1 -continuous finite element model, the number of unknowns is independent of the number of layers. The proposed finite element model is validated by comparing the present results with those obtained from the three-dimensional (3D) finite element analysis. In addition to correctly predicting the distribution of all stress components of the composite steel-concrete beams, the proposed finite element model is computationally economic.

Keywords: finite element; composite steel-concrete beams; refined high-order theory; transverse shear; normal stresses

1. Introduction

Due to the economic and structural advantages, composite steel-concrete structures are widely used throughout the world for the construction of buildings and bridges. Composite steel-concrete beams are the most common applications of the composite structures which are typically made of concrete slabs cast on steel members. Taking the advantage of the concrete in compression and steel in tension, composite steel-concrete beams have enhanced stiffness and strength performances in comparison to each components considered in isolation.

Various models have been presented in the literature to date for the analysis of composite steel-concrete beams (Spacone and El-Tawil 2004). Most of these earlier studies are based on Euler–Bernoulli’s beam theory. As an example, Li *et al.* (2014) introduced an exact dynamic stiffness method for investigating the free vibration characteristics of the composite steel-concrete beams. They employed the Euler–Bernoulli beam theory to define the dynamic behaviors of the composite beams. Although the Euler–Bernoulli hypothesis is very successful in the prediction of global responses (e.g., deflection, fundamental natural frequency or buckling load) of slender

*Corresponding author, Ph.D., E-mail: m.lezgy@hsu.ac.ir

homogeneous beams, it fails in the prediction of local behavior (e.g., through the thickness distribution of transverse shear and normal stresses, high natural frequencies) due to the neglecting of the transverse shear stress. Moreover, the transverse shear stress affects on the global response of beams having small length to thickness ratio, low shear rigidity or continuous spans (Ranzi and Zona 2007a). In order to incorporate the effect of shear stress in the analysis, some researchers (Berczynski and Wroblewski 2005, Xu and Wu 2007a, Schnabl *et al.* 2007) used Timoshenko's beam theory for the analysis of composite steel-concrete beams. Ranzi and colleagues (Ranzi and Zona 2007b, Ranzi 2008, Ranzi *et al.* 2010, Zona and Ranzi 2011) used a combination of Euler-Bernoulli's beam theory and Timoshenko's beam theory to analyze composite steel-concrete beams. They used Euler-Bernoulli's beam theory to model the concrete slab while the steel girders were modeled using Timoshenko's beam theory.

Although Timoshenko's beam theory leads to more accurate results in comparison to Euler-Bernoulli's beam theory, it gives a uniform shear stress distribution over the beam thickness whereas the actual variation of shear stress is parabolic. In order to remove this drawback of Timoshenko's beam theory, some researchers modified the shear stiffness of the beams by employing a shear correction factor. This factor which is dependent on the cross-sectional area of the beam, has a different value depending on the geometry and material properties of the beam. Under the action of static loads, Whitney (1973) evaluated shear correction factors of multilayered rectangular composite laminated beams. However, an accurate estimation of the shear correction factor is a complex procedure. Moreover, an analysis based on Timoshenko's beam theory cannot accurately predict the local responses of composite beams especially the distribution of the transverse shear and normal stresses. In order to overcome these limitations, several high-order beam theories have been presented in the literature to date. These high-order theories contain the third-order shear deformation theory (Reddy 2004), layer-wise or discrete-layer theories (Reddy 1987, Reddy *et al.* 1989, Barbero *et al.* 1990, Robbins and Reddy 1993), zig-zag theories (Ren 1986, Ren and Owen 1989, Whitney 1969, Icardi 1998, 2001a, b), global-local theories (Li and Liu 1997, Lezgy-Nazargah *et al.* 2011a, b) and mixed theories (Carrera 2000, 2001).

Although high-order theories are able to predict the local responses of composite beams accurately, they are often used for the analysis of multilayered laminated composite structure with rectangular cross-section. To the author's knowledge, none of these high-order theories has been applied for the analysis of composite steel-concrete beams. To fill this gap, in the present study, a refined high-order theory is employed for the analysis of composite steel-concrete beams. This theory which is based on global-local assumptions has been introduced first time by Lezgy-Nazargah *et al.* (2011b) for the analysis of laminated composite beams. The original high-order global-local theory then successfully extended to smart laminated composites by Lezgy-Nazargah and colleagues (Beheshti-Aval and Lezgy-Nazargah 2012, 2013, Beheshti-Aval *et al.* 2013). In this refined high-order theory, the global in-plane displacement component is described by combinations of polynomial and exponential expressions whereas the global transverse displacement component is adopted as a fourth-order polynomial. To improve the results, local terms have been added to the global expressions employing the discrete layer concepts. The employed high-order global-local theory considers effects of the transverse normal stress and transverse flexibility in the analysis. Majority of the available high-order theories either do not consider the transverse flexibility or do not impose the continuity condition of the transverse normal stress at the layer interfaces. However, the transverse normal stresses and strains and the transverse flexibility which are the cause of many failure modes, have important roles in the analysis of the laminated composite structures. In the employed high-order theory, the

boundary conditions of shear and normal tractions are also satisfied on the upper and lower surfaces of the beam. Besides, continuity conditions of the displacement components, transverse shear and normal stresses at the layer interfaces are satisfied. In comparison with the other available similar theories (layer-wise or 3D models available in the commercial softwares), the employed high-order theory is computationally significantly economic and has finally, only four independent generalized unknown parameters (three displacement and one rotation parameters). In this framework, the present study is focused on the extension of these last works to the analysis of composite steel-concrete beams.

Based on the high-order global-local theory, a three node beam element with C^0 -continuity for the in-plane displacements and C^1 -continuity for in-plane variations of the lateral deflection is employed. Various composite concrete-steel beams are treated using a written computer code whose algorithm is based on the present model. The obtained numerical results exhibit a good agreement with the 3D finite element (ABAQUS) results.

2. Theoretical formulation

2.1 The geometric parameters and the coordinate system

Fig. 1(a) shows the cross-section of a prismatic composite steel-concrete beam made of a concrete slab and a steel member. The geometric parameters of the composite beam and the chosen Cartesian coordinate system (x, y, z) are also shown in Fig. 1(b). As it may be noted from Fig. 1, the x, y and z axes are respectively along the length, width and thickness of the composite steel-concrete beam. In the present study it is assumed that the interface between the concrete slab and steel member is perfectly bonded. The study of the interlayer slip (partial interaction) between the steel and concrete slab is out of the scope of this work.

The original cross-section of Fig. 1(a) can be converted into the equivalent laminate section of Fig. 1(b). To this end, the original elastic moduli of each portion of the composite steel-concrete beam is replaced with the equivalent one of $\bar{E}^{(k)} = E^{(k)}b_k$ (k denotes the layer number of the beam). The height of each portion of steel-concrete beam is retained without any change in the equivalent laminate section. Following these changes, the composite beams with the cross-section of Fig. 1(a) and ones with the cross-section of Fig. 1(b) will have an identical axial and flexural stiffness. Thus, the two sections shown in Fig. 1 are equivalent in the one-dimensional beam

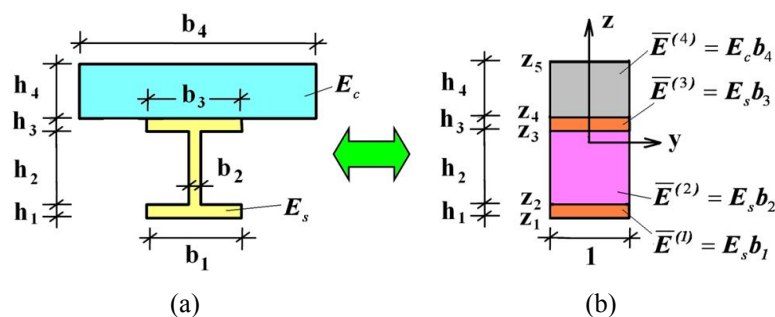


Fig. 1 (a) Typical cross-section of the composite beam; (b) Equivalent laminated cross-section of the composite beam

theory. To obtain the stress components at a point located in the original cross section of the composite beam, one must multiply by $1/b_k$ the stress computed at the corresponding point of the transformed section. The above described procedure for converting a composite steel-concrete beam section into an equivalent laminated one was also employed by Xu and Wu (2007b) for the two-dimensional analysis of simply supported composite steel-concrete beams. It is worthy to note that the described conversion of cross-section may be inadequate for problems with significant shear lag (e.g., for beams with wide flanges). Study of shear lag is not considered in this work.

2.2 The constitutive equations

In a laminated beam with small width, the 3D linear constitutive equations of the k th layer can be reduced to

$$\sigma^{(k)} = \bar{C}^{(k)} \varepsilon^{(k)} \quad (1)$$

where

$$\sigma^{(k)} = \begin{bmatrix} \sigma_{11}^{(k)} \\ \sigma_{33}^{(k)} \\ \tau_{13}^{(k)} \end{bmatrix}, \quad \varepsilon^{(k)} = \begin{bmatrix} \varepsilon_{11}^{(k)} \\ \varepsilon_{33}^{(k)} \\ \gamma_{13}^{(k)} \end{bmatrix}$$

$$\bar{C}^{(k)} = \begin{bmatrix} \bar{c}_{11}^{(k)} & \bar{c}_{12}^{(k)} & 0 \\ \bar{c}_{12}^{(k)} & \bar{c}_{22}^{(k)} & 0 \\ 0 & 0 & \bar{c}_{33}^{(k)} \end{bmatrix} = \begin{bmatrix} c_{11}^{(k)} & c_{13}^{(k)} & 0 \\ c_{13}^{(k)} & c_{33}^{(k)} & 0 \\ 0 & 0 & c_{55}^{(k)} \end{bmatrix}$$

$$- \begin{bmatrix} c_{16}^{(k)} & 0 & c_{12}^{(k)} \\ c_{36}^{(k)} & 0 & c_{23}^{(k)} \\ 0 & c_{45}^{(k)} & 0 \end{bmatrix} \begin{bmatrix} c_{66}^{(k)} & 0 & c_{26}^{(k)} \\ 0 & c_{44}^{(k)} & 0 \\ c_{26}^{(k)} & 0 & c_{22}^{(k)} \end{bmatrix}^{-1} \begin{bmatrix} c_{16}^{(k)} & c_{36}^{(k)} & 0 \\ 0 & 0 & c_{45}^{(k)} \\ c_{12}^{(k)} & c_{23}^{(k)} & 0 \end{bmatrix}$$

and k denotes the layer number and $c_{ij}^{(k)}$ are the elastic coefficients.

2.3 The displacement field description

In the present study, the following refined high-order global-local displacement field is employed ($k = 1, 2, \dots, N$) (Lezgy-Nazargah *et al.* 2011b)

$$u(x, y, z, t) = u_0(x, t) - zw_0(x, t)_{,x} + (\theta(x, t) + w_0(x, t)_{,x})J(z) + T(z)u_1^1(x, t) + P(z)X^+(x, t) + R(z)X^-(x, t) \quad (2)$$

$$w(x, y, z, t) = w_0(x, t) + \Delta_1^k(z)u_0(x, t)_{,x} + \Delta_2^k(z)w_0(x, t)_{,xx} + \Delta_3^k(z)\theta(x, t)_{,x} + \Delta_4^k(z)u_1^1(x, t)_{,x} + \Delta_5^k(z)X^+(x, t)_{,x} + \Delta_6^k(z)X^-(x, t)_{,x} + \Delta_7^k(z)Z^+(x, t) + \Delta_8^k(z)Z^-(x, t)$$

where the functions $u(x, y, z, t)$ and $w(x, y, z, t)$ represent the in-plane and transverse displacement components, respectively. $u_0(x, t)$ and $w_0(x, t)$ are global displacement parameters at the reference

plane. t is the time and $\theta(x, t)$ denotes the shear-bending rotation around the y axis. $u_1^1(x, t)$ is the local in-plane displacement parameter of the first layer of the laminated beam. $X^-(x, t)$ and $X^+(x, t)$ are the prescribed shear tractions of the bottom and top surfaces of the beam, respectively. $Z^-(x, t)$ and $Z^+(x, t)$ denote the distributed lateral loads acting on the bottom and top surfaces of the beam, respectively. In the context of coupled refined high-order global-local theory we have also

$$\begin{aligned}
 J(z) &= ze^{-2(z/h)^2} \\
 &+ \sum_{k=1}^{N_l} \left(\bar{z}_k \alpha_1^k + \left(-\frac{1}{2} + \frac{3\bar{z}_k^2}{2} \right) \alpha_2^k + \left(-\frac{3\bar{z}_k}{2} + \frac{5\bar{z}_k^3}{2} \right) \alpha_3^k \right) (H(z-z_k) - H(z-z_{k+1})) \\
 T(z) &= \sum_{k=1}^{N_l} \left(\bar{z}_k \beta_1^k + \left(-\frac{1}{2} + \frac{3\bar{z}_k^2}{2} \right) \beta_2^k + \left(-\frac{3\bar{z}_k}{2} + \frac{5\bar{z}_k^3}{2} \right) \beta_3^k \right) \times (H(z-z_k) - H(z-z_{k+1})) \\
 P(z) &= \sum_{k=1}^{N_l} \left(\bar{z}_k \delta_1^k + \left(-\frac{1}{2} + \frac{3\bar{z}_k^2}{2} \right) \delta_2^k + \left(-\frac{3\bar{z}_k}{2} + \frac{5\bar{z}_k^3}{2} \right) \delta_3^k \right) \times (H(z-z_k) - H(z-z_{k+1})) \\
 R(z) &= \sum_{k=1}^{N_l} \left(\bar{z}_k \lambda_1^k + \left(-\frac{1}{2} + \frac{3\bar{z}_k^2}{2} \right) \lambda_2^k + \left(-\frac{3\bar{z}_k}{2} + \frac{5\bar{z}_k^3}{2} \right) \lambda_3^k \right) \times (H(z-z_k) - H(z-z_{k+1})) \\
 \Delta_1^k(z) &= \Theta_{11}^1 z + \Theta_{21}^2 z^2 + \Theta_{31}^3 z^3 + \Theta_{41}^4 z^4 \\
 &+ \sum_{j=1}^{k-1} D_1^j (z-z_{j+1}) H(z-z_{j+1}) + \sum_{j=1}^{k-1} C_1^j (z-z_{j+1})^2 H(z-z_{j+1}) \\
 \Delta_2^k(z) &= \Theta_{12}^1 z + \Theta_{22}^2 z^2 + \Theta_{32}^3 z^3 + \Theta_{42}^4 z^4 \\
 &+ \sum_{j=1}^{k-1} D_2^j (z-z_{j+1}) H(z-z_{j+1}) + \sum_{j=1}^{k-1} C_2^j (z-z_{j+1})^2 H(z-z_{j+1}) \\
 \Delta_3^k(z) &= \Theta_{13}^1 z + \Theta_{23}^2 z^2 + \Theta_{33}^3 z^3 + \Theta_{43}^4 z^4 \\
 &+ \sum_{j=1}^{k-1} D_3^j (z-z_{j+1}) H(z-z_{j+1}) + \sum_{j=1}^{k-1} C_3^j (z-z_{j+1})^2 H(z-z_{j+1}) \\
 \Delta_4^k(z) &= \Theta_{14}^1 z + \Theta_{24}^2 z^2 + \Theta_{34}^3 z^3 + \Theta_{44}^4 z^4 \\
 &+ \sum_{j=1}^{k-1} D_4^j (z-z_{j+1}) H(z-z_{j+1}) + \sum_{j=1}^{k-1} C_4^j (z-z_{j+1})^2 H(z-z_{j+1}) \\
 \Delta_5^k(z) &= \Theta_{15}^1 z + \Theta_{25}^2 z^2 + \Theta_{35}^3 z^3 + \Theta_{45}^4 z^4 \\
 &+ \sum_{j=1}^{k-1} D_5^j (z-z_{j+1}) H(z-z_{j+1}) + \sum_{j=1}^{k-1} C_5^j (z-z_{j+1})^2 H(z-z_{j+1}) \\
 &\downarrow
 \end{aligned} \tag{3}$$

$$\begin{aligned}
& \uparrow \\
\Delta_6^k(z) &= \Theta_{16}^1 z + \Theta_{26}^2 z^2 + \Theta_{36}^3 z^3 + \Theta_{46}^4 z^4 \\
& \quad + \sum_{j=1}^{k-1} D_6^j (z - z_{j+1}) H(z - z_{j+1}) + \sum_{j=1}^{k-1} C_6^j (z - z_{j+1})^2 H(z - z_{j+1}) \\
\Delta_7^k(z) &= \Theta_{17}^1 z + \Theta_{27}^2 z^2 + \Theta_{37}^3 z^3 + \Theta_{47}^4 z^4 \\
& \quad + \sum_{j=1}^{k-1} D_7^j (z - z_{j+1}) H(z - z_{j+1}) + \sum_{j=1}^{k-1} C_7^j (z - z_{j+1})^2 H(z - z_{j+1}) \\
\Delta_8^k(z) &= \Theta_{18}^1 z + \Theta_{28}^2 z^2 + \Theta_{38}^3 z^3 + \Theta_{48}^4 z^4 \\
& \quad + \sum_{j=1}^{k-1} D_8^j (z - z_{j+1}) H(z - z_{j+1}) + \sum_{j=1}^{k-1} C_8^j (z - z_{j+1})^2 H(z - z_{j+1})
\end{aligned} \tag{3}$$

In the above equations, H denotes Heaviside's function. $\alpha_1^k, \alpha_2^k, \alpha_3^k, \beta_1^k, \beta_2^k, \beta_3^k, \delta_1^k, \delta_2^k, \delta_3^k, \lambda_1^k, \lambda_2^k, \lambda_3^k$ are coefficients which appear from fulfillment of the inter-laminar continuity conditions of the transverse shear stress on the interfaces between the layers, and its boundary conditions on the upper and lower surfaces of the beam. The coefficients $C_1^k, C_2^k, C_3^k, C_4^k, C_5^k, C_6^k, C_7^k, C_8^k, D_1^k, D_2^k, D_3^k, D_4^k, D_5^k, D_6^k, D_7^k, D_8^k, \Theta_{11}^k, \Theta_{12}^k, \Theta_{13}^k, \Theta_{14}^k, \Theta_{15}^k, \Theta_{16}^k, \Theta_{17}^k$ and Θ_{18}^k ($l = 1, 2, 3, 4$) can be obtained by imposing the continuity conditions of the transverse normal stress and transverse normal stress gradient at $N_l - 1$ interfaces, and their boundary conditions on the upper and lower faces of the beam. It is worthy to note that these coefficients are only dependent on the material properties and the global coordinates of the layers. These coefficients can be easily calculated using a symbolic calculator software based on the procedure hinted in reference (Lezgy-Nazargah *et al.* 2011b). It is seen from Eq. (2) that the employed theory represent the in-plane and transverse displacement of the laminated beam with respect to four unknowns parameters u_0, w_0, θ and u_1^1 . Indeed, the employed high-order theory has only one generalized unknown parameter more than Timoshenko's beam theory.

Using Cauchy's definition of the strain tensor, the in-plane, transverse shear and normal strain components may be calculated based on the employed coupled global-local description of the displacement field as

$$\begin{aligned}
\varepsilon_{xx} &= u_{0,x} - z w_{0,xx} + (\theta_{,x} + w_{0,xx}) J(z) + T(z) u_{1,x}^1 + P(z) (X^+)_{,x} + R(z) (X^-)_{,x} \\
\varepsilon_{zz} &= \Delta_1^k(z)_{,z} u_{0,x} + \Delta_2^k(z)_{,z} w_{0,xx} + \Delta_3^k(z)_{,z} \theta_{,x} + \Delta_4^k(z)_{,z} (u_1^1)_{,x} + \Delta_5^k(z)_{,z} (X^+)_{,x} \\
& \quad + \Delta_6^k(z)_{,z} (X^-)_{,x} + \Delta_7^k(z)_{,z} Z^+ + \Delta_8^k(z)_{,z} Z^- \\
\gamma_{xz} &= (\theta + w_{0,x}) J(z)_{,z} + T(z)_{,z} u_1^1 + P(z)_{,z} X^+ + R(z)_{,z} X^-
\end{aligned} \tag{4}$$

2.4 Finite element formulation

A three noded beam element is developed based on the employed refined high-order global-local theory. As the highest derivative of w_0 in the expression of the strain energy is of second-order, this variable interpolated using C^1 -continuous Hermite cubic shape functions. Although the rotation θ can be C^0 -continuous, it is interpolated by quadratic Lagrangian shape functions to ensure obtaining more accurate results. Finally, $u_0, u_1^1, X^+, X^-, Z^+$ and Z^- are

interpolated using Lagrangian quadratic shape functions. Based on Eqs. (2) and (4), the displacement and strain components may be expressed in the following matrix form

$$u = A_u u_u, \quad \varepsilon = L_u u_u \tag{5}$$

where $u = [u \ w]^T$, $u_u = [u_0 \ w_0 \ \theta \ u_1^1 \ X^+ \ X^- \ Z^+ \ Z^-]^T$ and $\varepsilon = [\varepsilon_{xx} \ \varepsilon_{zz} \ \gamma_{xz}]^T$. The displacement vector of the reference layer u_u may be expressed in terms of the nodal variables vector u_u^e as follows

$$u_u = N_u u_u^e \tag{6}$$

where

$$u_u^e = \left\{ (u_0)_1 \ (w_0)_1 \ \theta_1 \ (w_{0,x})_1 \ (u_1^1)_1 \ (X^+)_1 \ (X^-)_1 \ (Z^+)_1 \ (Z^-)_1 \ (u_0)_3 \ \theta_3 \ (u_1^1)_3 \right. \\ \left. (X^+)_3 \ (X^-)_3 \ (Z^+)_3 \ (u_0)_2 \ (w_0)_2 \ \theta_2 \ (w_{0,x})_2 \ (u_1^1)_2 \ (X^+)_2 \ (X^-)_2 \ (Z^+)_3 \ (Z^-)_3 \right\}^T$$

For the sake of brevity, the expression for A_u , L_u and N_u are not presented here. The interested readers can refer to reference (Lezgy-Nazargah *et al.* 2011b) for more details. Using Eq. (6), the displacements and the strain vectors may be expressed as follows

$$u = A_u u_u = A_u N_u u_u^e = \mathcal{N} u_u^e \tag{7}$$

$$\varepsilon = L_u u_u = L_u N_u u_u^e = \mathcal{D}_u u_u^e \tag{8}$$

The principle of virtual displacement is employed to extract the governing equations of the composite beam element. According to this principle, for a mechanical medium with volume Ω and regular boundary surfaces Γ , one may write

$$\delta \Pi = \delta U - \delta W = \int_{\Omega} \delta \varepsilon^T \sigma \, d\Omega - \int_{\Gamma} \delta u^T F \, dS - \int_{\Omega} \delta u^T f \, d\Omega - \delta u_c^T f_c + \int_{\Omega} \rho \delta u^T \ddot{u} \, d\Omega = 0 \tag{9}$$

Where δu , F , f , and f_c are the admissible virtual displacement, traction, body force, and concentrated force vectors, respectively. U , W , and ρ are the strain energy, work of the externally applied loads, and mass density, respectively.

Substituting Eqs. (1) and (8) into Eq. (9), and assembling the element matrices, the following general equations of motion are obtained for the entire composite steel-concrete beam

$$\mathcal{M} \ddot{u}(t) + \mathcal{K} u(t) = \mathcal{F}(t) \tag{10}$$

where

$$\mathcal{M} = \int_{\Omega} \rho \mathcal{N}^T \mathcal{N} \, d\Omega$$

$$\mathcal{K} = \int_{\Omega} \mathcal{D}_u^T \bar{C} \mathcal{D}_u \, d\Omega$$

$$\mathcal{F} = \int_{\Omega} \mathcal{N}^T f \, dV + \int_{\Gamma} \mathcal{N}^T F \, dS + \mathcal{N}^T f_c$$

3. Numerical results and discussions

In order to evaluate the performance of the proposed finite element model, the static analysis of some composite steel-concrete beams is considered in this section. A computer code is developed in MATLAB to implement the proposed model which is used to generate results. A composite steel-concrete beam with various boundary conditions has been analyzed using the proposed model. As there is no result based on high-order beam theory available in the literature for the present problem, the present results are compared with the finite elements results obtained based on the 3D theory of elasticity. The 3D finite element analysis is performed using the 20-node solid element (C3D20RE) available in ABAQUS software with a very refined mesh.

3.1 Example 1

In the current example, a simply supported (S-S) composite steel-concrete beam with the length $L = 6$ m is analyzed using the proposed finite element formulation. The geometric parameters of the composite beam are shown in Fig. 2. A distributed uniform pressure with the magnitude $Z^+ = 10$ kN/m² is applied on the top of the composite beam. The elastic moduli and Poisson's ratios are $E_c = 8.5$ GPa, $\nu_c = 0.2$, $E_s = 210$ GPa and $\nu_s = 0.3$ for concrete and steel, respectively. The mesh convergence study shows that a mesh with 20 elements (329 dof) of equal lengths is adequate to model the composite steel-concrete beam. Since no exact 3D solution is available for the considered example, a 3D finite element analysis was performed in ABAQUS/CAE Version 6.8-3. ABAQUS/CAE provides a graphical environment that allows for easy modeling of complex geometry. It was assumed that the concrete slab and steel member can be modeled as a quadratic 20-node brick element (solid element). The mesh with 10980 elements (about 52000 dofs) shown in Fig. 3 yields converged results for both global and local responses. They will be considered as a reference. Boundary and loading conditions can be also easily assigned to the generated geometry in ABAQUS/CAE. At the two ends of the composite beam, the transverse deflection of the concrete slab and steel member along z -axis is restrained ($w = Uz = 0$). A uniform pressure was also applied on the top of the composite beam (along z -axis) in the ABAQUS model.

Through-the-thickness variations of the displacement and stress components are shown in Fig. 4. It may be readily seen from Fig. 4 that the proposed finite element model predicts the in-plane stress very accurately. The transverse shear stress distribution obtained from the present model is in good agreement with the ABAQUS results. Both models give similar results except at the region near to the interface of the layers. As it was expected, the presented model predicts the transverse normal deflection of the composite beam with sufficient accuracy (the maximum error

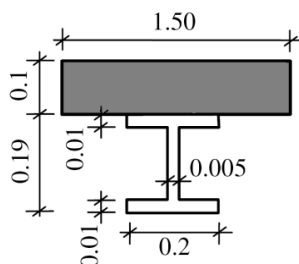


Fig. 2 Cross section of the composite steel-concrete beam of example 1

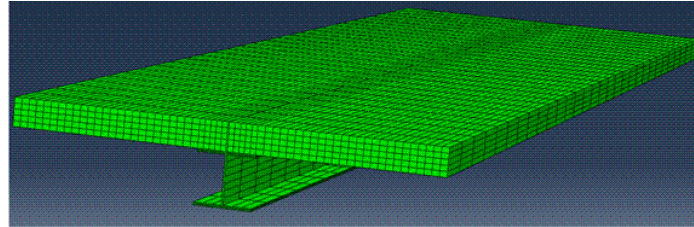
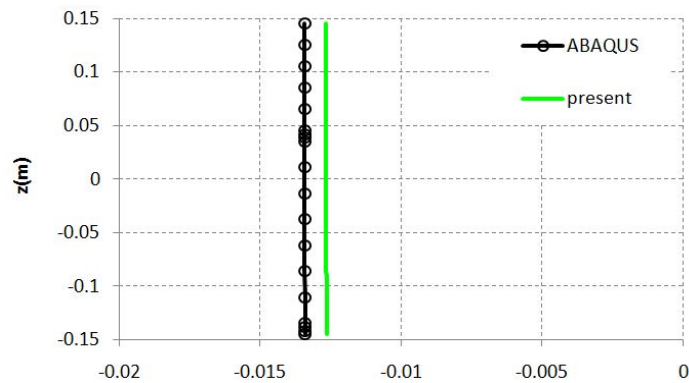
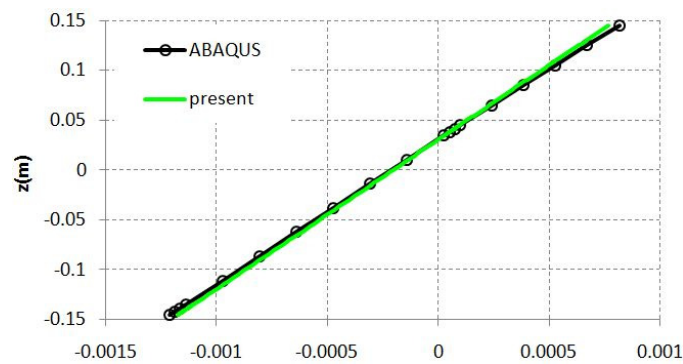


Fig. 3 Composite steel-concrete beam; mesh with 10980 elements (ABAQUS)

is about 5.7%). The obtained results also show that the presented model predicts the in-plane displacement of the composite beam with an error that is less than 6%. The transverse normal stress calculated based on the present model is compared well with the 3D finite element results with a relative error of 8.3%. Fig. 4 shows that the values of transverse normal stress are relatively noticeable and should be considered in the design of composite steel-concrete beams. The maximal value of the transverse normal stress occurs at the interface of the top flange and the web of the steel member.

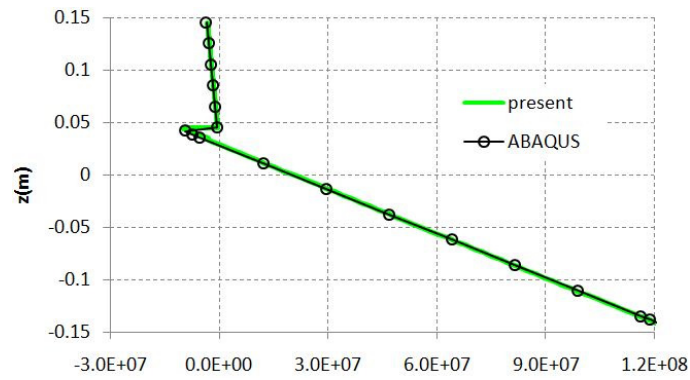


(a) Transverse deflection at $(L/2, z)$

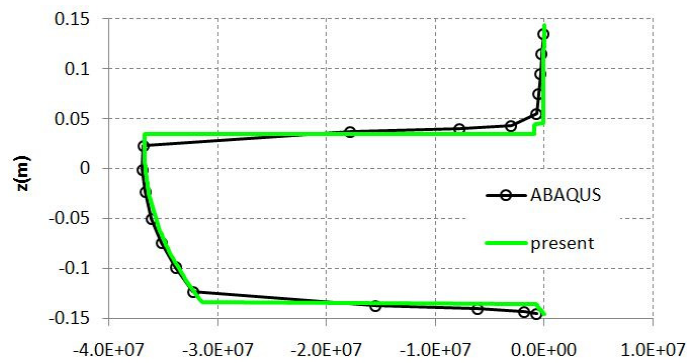


(b) In-plane displacement at $(0, z)$

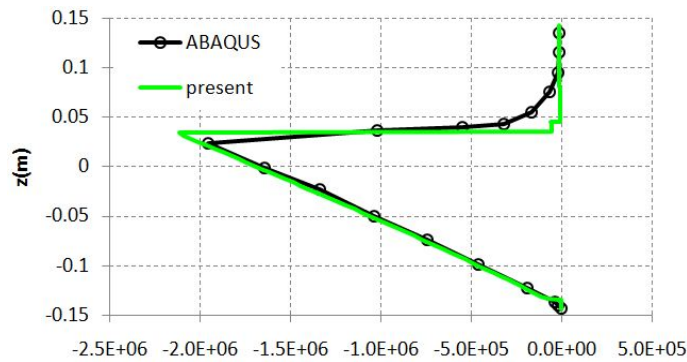
Fig. 4 Through-the-thickness distribution of w (m), u (m), σ_{xx} (N/m²), τ_{xz} (N/m²) and σ_{zz} (N/m²) for the simply supported composite steel-concrete beam



(c) In-plane stress at $(L/2, z)$



(d) Transverse shear stress at $(0, z)$



(e) Transverse normal stress at $(L/2, z)$

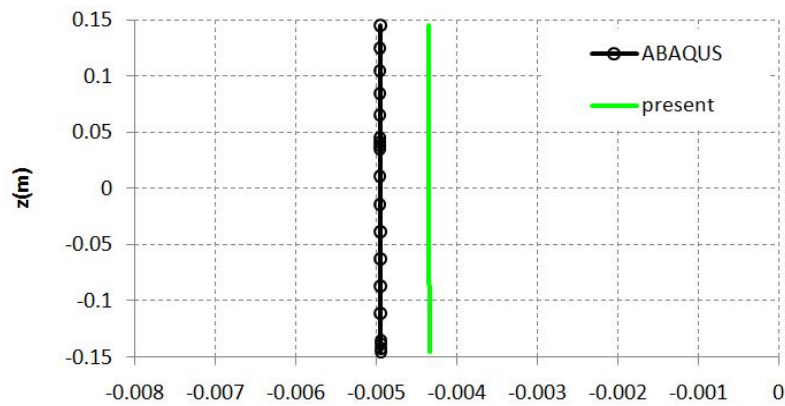
Fig. 4 Continued

It can be deduced from these results that the proposed model is able to predict the local responses of the composite steel-concrete beams with sufficient accuracy. However, the converged mesh of the 3D finite element model (ABAQUS) has about 52000 degrees of freedom while the proposed finite element formulation needs only 329 degrees of freedom.

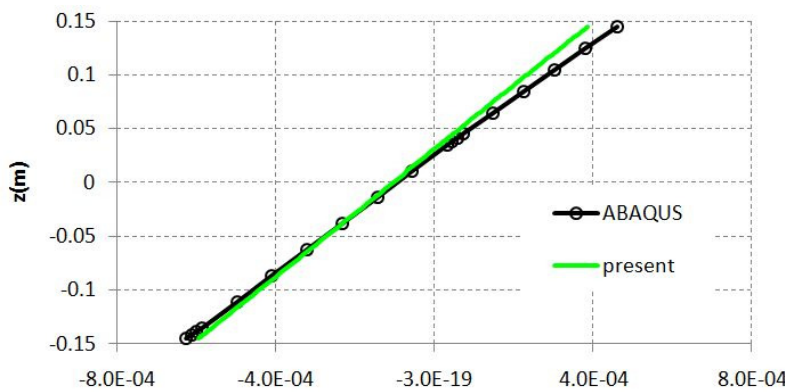
3.2 Example 2

In this section, the capability of the present finite element model for the analysis of the composite steel-concrete beams with different boundary conditions is evaluated. To this end, the composite beams with clamped-simply supported (C-S) and clamped-clamped (C-C) end conditions are analyzed using the present finite element. The geometric parameters, loading conditions and the material properties of the considered beams of the present example are the same as those of the previous example. The accuracy of the present results is assessed in comparison with the results obtained from ABAQUS. It is worthy to note that in the ABAQUS model, all the three displacement degrees of freedom of the concrete slab and steel member were restrained ($u = Ux = 0, v = Uy = 0, w = Uz = 0$) at each clamped end.

Through-the-thickness distributions of the stress and displacement components along the thickness direction are shown in Figs. 5 and 6. Similar to the previous example, the results obtained from the present finite element are in good agreement with ABAQUS results. The present



(a) Transverse deflection at $(L/4, z)$



(b) In-plane displacement at (L, z)

Fig. 5 Through-the-thickness distribution of w (m), u (m), σ_{xx} (N/m²), τ_{xz} (N/m²) and σ_{zz} (N/m²) for the composite steel-concrete beam with C-S end conditions

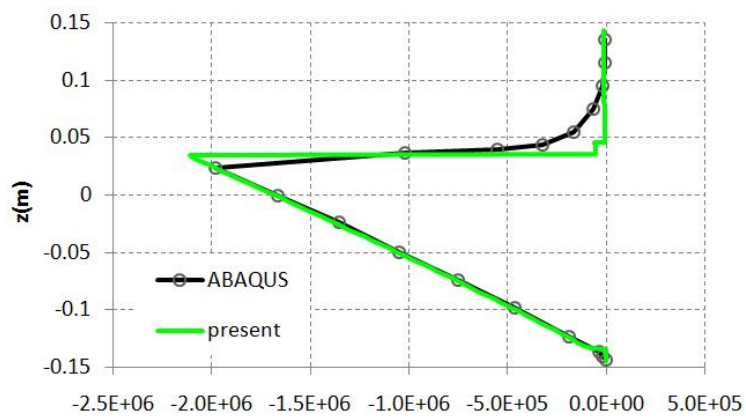
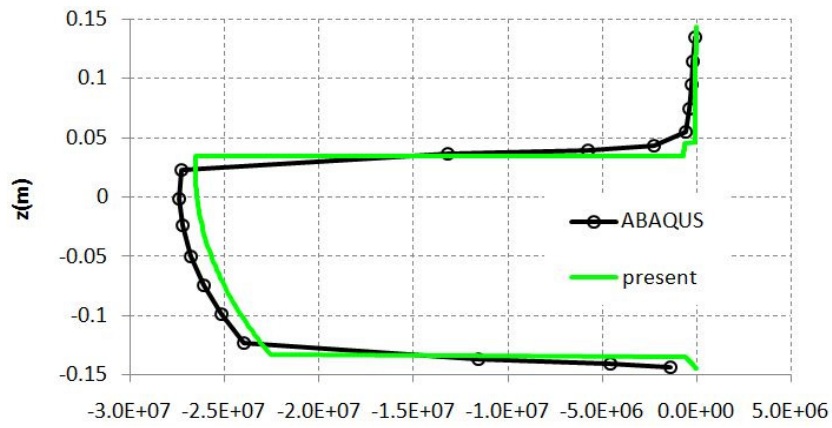
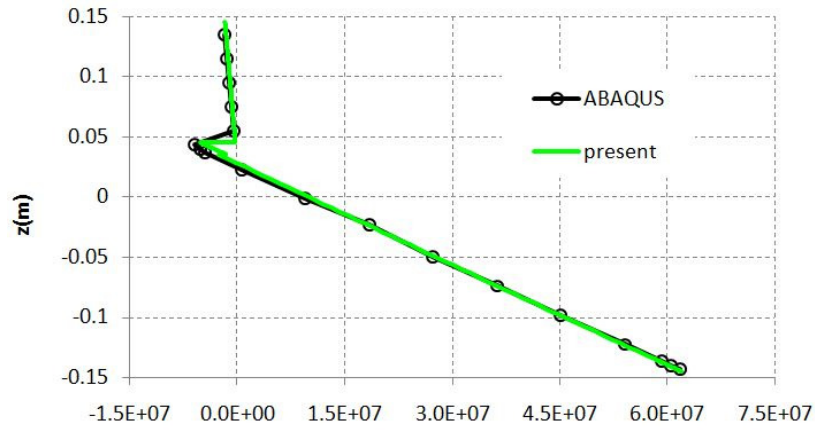
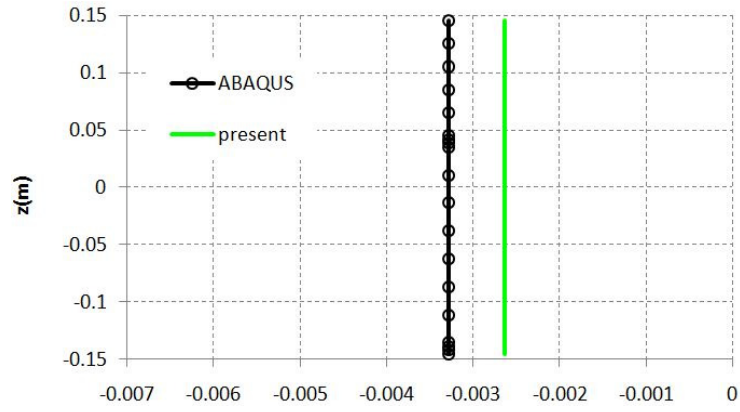
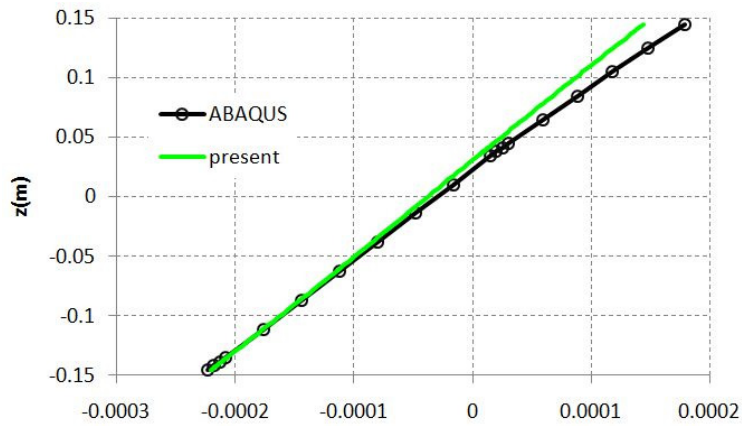


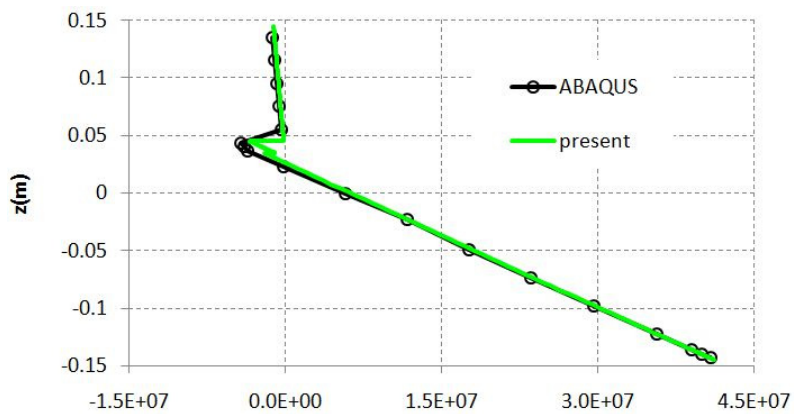
Fig. 5 Continued



(a) Transverse deflection at $(L/2, z)$



(b) In-plane displacement at $(L/4, z)$



(c) In-plane stress at $(L/2, z)$

Fig. 6 Through-the-thickness distribution of w (m), u (m), σ_{xx} (N/m²), τ_{xz} (N/m²) and σ_{zz} (N/m²) for the composite steel-concrete beam with C-C end conditions

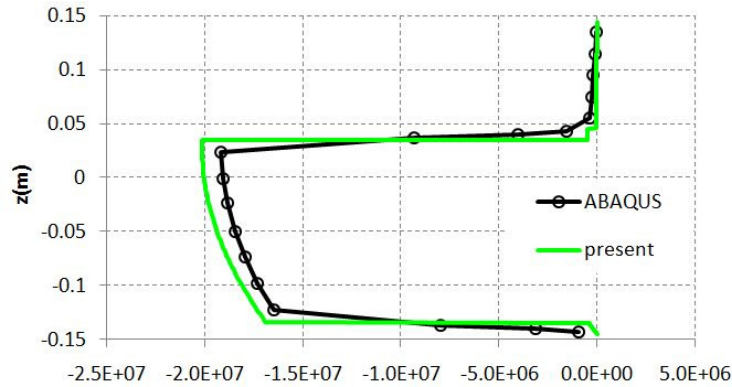
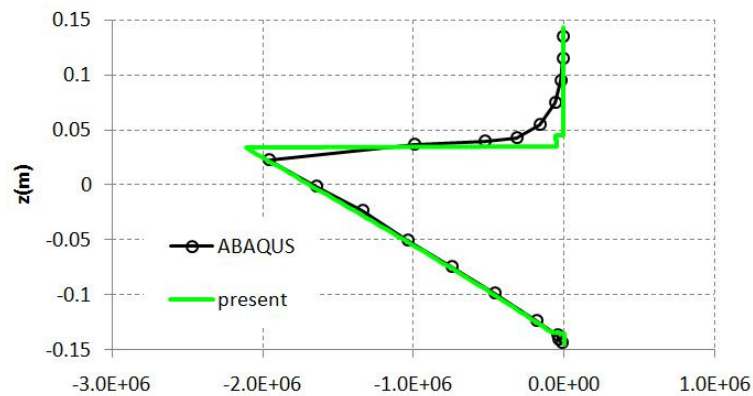
(d) Transverse shear stress at $(L/4, z)$ (e) Transverse normal stress at $(L/2, z)$

Fig. 6 Continued

finite element predicts the in-plane stress of the composite beams with C-S and C-C end conditions very accurately. Concerning the transverse shear stress, the present model gives results with the error less than 5%. The proposed finite element model predicts the transverse normal stress of the composite beam with C-S end conditions within a 6.7 % error. In case of C-C end conditions, this value is 7.8%. Obtained numerical results show that the error corresponding to the present finite element model is higher for C-S beam than for S-S beam, and higher for C-C beam than for S-C. Nevertheless, the error rate in the prediction of stress components of the composite beam is less than 8% regardless of the mechanical boundary conditions.

It can be observed from Figs. 5 and 6 that the predicted distribution of in-plane and transverse displacement obtained from the present model is similar to ABAQUS computations. Although the differences are mainly due to using different solution procedures, the present high order global-local approximation of the displacement components has improved the prediction of the in-plane and transverse displacement of the composite beam, considerably. Moreover, the present finite element is computationally very low cost in comparison to the 3D finite element model.

These obtained numerical results demonstrate the efficiency of the proposed finite element in

the prediction of local behaviors of composite steel-concrete beams with different boundary conditions.

4. Conclusions

An efficient finite element is presented for the analysis of composite steel-concrete beams. The kinematics is based on a refined high-order beam theory which satisfies all the kinematic and stress boundary conditions at the layers interfaces. In contrast to the most of available theories, the employed high-order theory takes into account the effects of the transverse normal stress and the transverse flexibility of the beam. In the proposed finite element formulation, the number of the unknown parameters is very small and is independent of the number of the layers. Moreover, the proposed model does not need any shear correction factor.

In order to assess the accuracy of the proposed finite element for the static analysis of composite steel-concrete beams, comparisons have been made with the results obtained from the 3D finite element analysis. To this purpose, composite beams with various boundary conditions are analyzed using the proposed finite element. The comparisons show that the presented finite element formulation is sufficiently accurate in the prediction of global and local behaviors of composite steel-concrete beams. However, the proposed model has only one generalized unknown parameter more than Timoshenko's beam theory. Compared to 3D elements available in the commercial softwares, only few degrees of freedom are needed to obtain good results with the present finite element. This approach seems to be a good compromise between computational cost and accuracy for the composite steel-concrete beams problem. More advanced problems are now investigated using this new finite element model, and special attention is pointed towards the shear-lag and interlayer slips effects.

References

- Barbero, E.J., Reddy, J.N. and Teply, J. (1990), "An accurate determination of stresses in thick laminates using a generalized plate theory", *Int. J. Numer. Method. Eng.*, **29**(1), 1-14.
- Beheshti-Aval, S.B. and Lezgy-Nazargah, M. (2012), "A coupled refined high-order global-local theory and finite element model for static electromechanical response of smart multilayered/sandwich beams", *Arch. Appl. Mech.*, **82**(12), 1709-1752.
- Beheshti-Aval, S.B. and Lezgy-Nazargah, M. (2013), "Coupled refined layerwise theory for dynamic free and forced response of piezoelectric laminated composite and sandwich beams", *Meccanica*, **48**(6), 1479-1500.
- Beheshti-Aval, S.B., Shahvaghari-Asl, S., Lezgy-Nazargah, M. and Noori, M. (2013), "A finite element model based on coupled refined high-order global-local theory for static analysis of electromechanical embedded shear-mode piezoelectric sandwich composite beams with various widths", *Thin-Wall. Struct.*, **72**, 139-163.
- Berczynski, S. and Wroblewski, T. (2005), "Vibration of steel-concrete composite beams using the Timoshenko beam model", *J. Vib. Control*, **11**(6), 829-848.
- Carrera, E. (2000), "An assessment of mixed and classical theories on global and local response of multilayered orthotropic plates", *Compos. Struct.*, **50**(2), 183-198.
- Carrera, E. (2001), "Developments, ideas and evaluations based upon Reissner's mixed variational theorem in the modeling of multilayered plates and shells", *Appl. Mech. Rev.*, **54**(4), 301-329.
- Icardi, U. (1998), "Eight-noded zig-zag element for deflection and stress analysis of plates with general

- lay-up”, *Compos. Part B*, **29**(4), 425-441.
- Icardi, U. (2001a), “A three-dimensional zig-zag theory for analysis of thick laminated beams”, *Compos. Struct.*, **52**(1), 123-135.
- Icardi, U. (2001b), “Higher-order zig-zag model for analysis of thick composite beams with inclusion of transverse normal stress and sublaminates approximations”, *Compos. Part B*, **32**(4), 343-354.
- Lezgy-Nazargah, M., Shariyat, M. and Beheshti-Aval, S.B. (2011a), “A refined high-order global-local theory for finite element bending and vibration analyses of the laminated composite beams”, *Acta Mech.*, **217**(3-4), 219-242.
- Lezgy-Nazargah, M., Beheshti-Aval, S.B. and Shariyat, M. (2011b), “A refined mixed global-local finite element model for bending analysis of multi-layered rectangular composite beams with small widths”, *Thin-Wall. Struct.*, **49**(2), 351-362.
- Li, X. and Liu, D. (1997), “Generalized laminate theories based on double superposition hypothesis”, *Int. J. Numer. Method. Eng.*, **40**(7), 1197-1212.
- Li, J., Huo, Q., Li, X., Kong, X. and Wu, W. (2014), “Dynamic stiffness analysis of steel-concrete composite beams”, *Steel Compos. Struct., Int. J.*, **16**(6), 577-593.
- Ranzi, G. (2008), “Locking problems in the partial interaction analysis of multi-layered composite beams”, *Eng. Struct.*, **30**(10), 2900-2911.
- Ranzi, G. and Zona, A. (2007a), “A composite beam model including the shear deformability of the steel component”, *Eng. Struct.*, **29**(11), 3026-3041.
- Ranzi, G. and Zona, A. (2007b), “A steel-concrete composite beam model with partial interaction including the shear deformability of the steel component”, *Eng. Struct.*, **29**(11), 3026-3041.
- Ranzi, G., Dall’Asta, A., Ragni, L. and Zona, A. (2010), “A geometric nonlinear model for composite beams with partial interaction”, *Eng. Struct.*, **32**(5), 1384-1396.
- Reddy, J.N. (1987), “A generalization of two-dimensional theories of laminated composite plates”, *Commun. Appl. Numer. Method.*, **3**(3), 173-180.
- Reddy, J.N. (2004), *Mechanics of Laminated Composite Plates and Shells: Theory and Analysis*, CRC Press, Boca Raton, FL, USA.
- Reddy, J.N., Barbero, E.J. and Teply, J. (1989), “A plate bending element based on a generalized laminate plate theory”, *Int. J. Numer. Method. Eng.*, **28**(10), 2275-2292.
- Ren, J.G. (1986), “Bending theory of laminated plates”, *Compos. Sci. Technol.*, **27**(3), 225-248.
- Ren, J.G. and Owen, D.R.J. (1989), “Vibration and buckling of laminated plates”, *Int. J. Solid. Struct.*, **25**(2), 95-106.
- Robbins Jr., D.H. and Reddy, J.N. (1993), “Modeling of thick composites using a layerwise laminate theory”, *Int. J. Numer. Method. Eng.*, **36**(4), 655-677.
- Schnabl, S., Saje, M., Turk, G. and Planinc, I. (2007), “Locking-free two-layer Timoshenko beam element with interlayer slip”, *Finite Elem. Anal. Des.*, **43**(9), 705-714.
- Spacone, E. and El-Tawil, S. (2004), “Nonlinear analysis of steel–concrete composite structures: State-of-the-art”, *J. Struct. Eng.*, **130**(2), 159-168.
- Whitney, J.M. (1969), “The effects of transverse shear deformation on the bending of laminated plates”, *J. Compos. Mater.*, **3**(3), 534-547.
- Whitney, J.M. (1973), “Shear correction factors for orthotropic laminates under static load”, *J. Appl. Mech. ASME*, **40**(1), 302-304.
- Xu, R.Q. and Wu, Y.F. (2007a), “Static, dynamic, and buckling analysis of partial interaction composite members using Timoshenko’s beam theory”, *Int. J. Mech. Sci.*, **49**(10), 1139-1155.
- Xu, R.Q. and Wu, Y.F. (2007b), “Two-dimensional analytical solutions of simply supported composite beams with interlayer slips”, *Int. J. Solids Struct.*, **44**(1), 165-175.
- Zona, A. and Ranzi, G. (2011), “Finite element models for non-linear analysis of steel concrete composite beams with partial interaction in combined bending and shear”, *Finite Elem. Anal. Des.*, **47**(2), 98-118.